lubricants

Article

Influence of Water Contamination, Iron Particles, and Energy Input on the NVH Behavior of Wet Clutches

Johannes Wirkner [1,*], Mirjam Baese [2], Astrid Lebel [3], Hermann Pflaum [1], Katharina Voelkel [1], Lukas Pointner-Gabriel [1], Charlotte Besser [3], Thomas Schneider [1] and Karsten Stahl [1]

1 Gear Research Center (FZG), Department of Mechanical Engineering, School of Engineering and Design, Technical University of Munich, Boltzmannstrasse 15, D-85748 Garching, Germany
2 Magna Powertrain GmbH & Co. KG, Industriestrasse 35, A-8502 Lannach, Austria
3 AC2T Research GmbH, Viktor-Kaplan-Strasse 2/C, A-2700 Wiener Neustadt, Austria
* Correspondence: johannes.wirkner@tum.de

Abstract: The driving comfort and safety of the automotive powertrain are significantly related to the performance, lifetime, and functionality of the lubricant. The presented study focuses on investigating the performance loss of the lubricant due to water contamination resulting from environmental influences and iron particles originating from the wear of different machine elements. The main purpose is to determine critical factors that contribute to the degradation of the lubricant, and increase the tendency to NVH behavior, leading to adverse comfort losses to the respective user. Therefore, this performance loss is evaluated by test rig-based analysis of the friction behavior of wet clutches. Due to physical adsorption, a significant impact of water and iron contamination on the degradation of the lubricant is found, while the influence of the energy input is secondary.

Keywords: wet clutch; shudder; NVH; water contamination; iron particles; energy input; friction behavior; lubrication; additives; ICP-OES

Citation: Wirkner, J.; Baese, M.; Lebel, A.; Pflaum, H.; Voelkel, K.; Pointner-Gabriel, L.; Besser, C.; Schneider, T.; Stahl, K. Influence of Water Contamination, Iron Particles, and Energy Input on the NVH Behavior of Wet Clutches. *Lubricants* **2023**, *11*, 459. https://doi.org/10.3390/lubricants11110459

Received: 31 July 2023
Revised: 23 October 2023
Accepted: 25 October 2023
Published: 27 October 2023

1. Introduction

Wet clutches are commonly used in manifold applications, including industrial machinery and automotive systems, where modulation and torque transmission are essential. The latter is mainly characterized by the friction behavior of wet clutches which cannot be numerically calculated due to various interactions of the tribological system consisting of lubricant, friction lining, steel disk, and operating conditions. Thus, experimental testing is required to determine the friction behavior of a specific clutch system. With respect to this, the presence of adverse effects to the driver, such as the occurrence of shudder leading to NVH (noise, vibration, and harshness) in the powertrain unit, can be avoided.

1.1. Motivation and State of the Art

In automotive applications, wet clutches are used in transfer cases to transmit the induced torque from the front to the rear axle [1]. Additionally, wet clutches contribute to a reduction in oscillations, for instance, in hybrid powertrain systems as geometrical asymmetries are compensated by their damping mode of action [2]. Due to the compact design and the occurrence of high torques, proficient heat dissipation is required, which makes the use of a cooling liquid inevitable.

Among various factors, such as the friction material, topography of the steel disk, mechanical and thermal stress, as well as initial damage, the friction behavior is significantly influenced by the interaction of the friction interfaces with the lubricant. Generally, the performance of the clutch system mainly depends on the friction behavior, which is primarily characterized by the course of the coefficient of friction (CoF) with respect to the sliding speed [3]. Ideally, the curve shows a desired, positive gradient ($\Delta\mu/\Delta v_s > 0$), resulting in good control behavior and, thus, no tendency to shudder. With a negative gradient or a static CoF that significantly exceeds the dynamic CoF ($\mu_0 >> \mu$), the control behavior turns poor, and the tendency to shudder rises. This directly leads to a loss of comfort to the acquirer of the respective application [4,5] as shown in Figure 1. Additionally, the induced vibrations cause an increased wear behavior of the friction disks [6]. To avoid the presence of these adverse effects, specific additives are used that improve the controllability of the entire powertrain unit. Generally, lubricants used in transmission systems serve as cooling fluid and require to fulfill different system needs. This involves anti-wear properties, foam performance, efficiency requirements, and durability demands. Furthermore, the performance criteria must be met, including, for instance, the friction behavior of wet clutches, which is shaped by the use of friction modifiers [7]. Previous studies have shown that adding detergent and dispersants, which are also used for oxidation stability, significantly increases the CoF for organic friction lining [8–10]. Friction modifiers, conversely, mostly consist of fatty acids, aliphatic, or phosphate esters and cause an inherent reduction in the static CoF [9,11]. Consequently, the tendency to a negative gradient of the CoF versus the sliding speed and, thus, the occurrence of shudder decreases [12,13]. Additionally, the influence of additives on the friction behavior and shudder tendency of wet clutches significantly depends on the operating parameters and the interaction of the friction material with the respective additive elements [8,14,15]. With increasing the lifetime and energy input, components of the friction modifier consecutively degrade, and thus, the performance of the lubricant deteriorates [5,14].

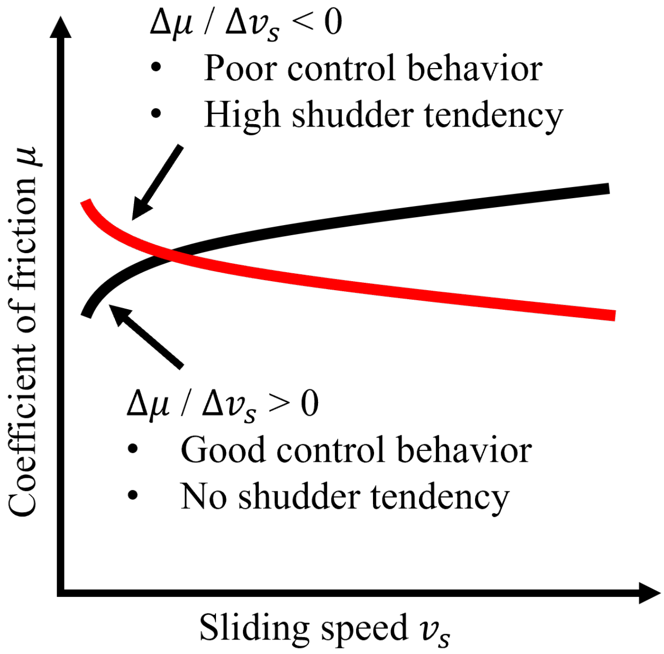

Figure 1. CoF with respect to the sliding speed based on Naunheimer et al. [3].

Besides lubricant aging via continuous energy input throughout the lifetime, environmental influences, such as water contamination, can contribute to an earlier performance loss of the lubricant. Various investigations have shown that water influences the tribological system of wet clutches by promoting an increased static CoF as well as a negative gradient of the $\mu - v_s$-relation [16–19]. These effects can persist far above the boiling point of water [20]. Baese et al. [1,21] examined via Time-of-Flight Secondary Ion Mass Spectrometry (ToF-SIMS) analyses that a water-contaminated lubricant can lead to changes in the tribo-layers of the steel disk. Additionally, physical adsorption between water molecules and additive elements can modify the structure of the latter and thus, inhibit the respective additive from complying with its initial purpose [22–25]. According to Williamson et al. [20], those changes can also be observed with regard to the friction material.

To find the root cause of NVH behavior obtained in transmission systems caused by water, various tests at component level were performed. While Wang et al. [18] applied a standardized SAE No. 2 test rig [26], other authors reduced the complexity of the system by using a simplified design, such as single-disk or pin-on-disk test rigs [16,19,20]. Williamson et al. [20] and Fatima et al. [16] described a defined run-in or brake-in procedure before determining the friction behavior via slip shift cycles consisting of an engagement and a cooling phase, respectively. Most of the time, the lubricant was supplied into the test rig already being pre-contaminated by a specific water amount [18,20]. Fatima et al. [16], however, added the designated water amount into the test rig after the run-in procedure. As the desired friction behavior was obtained, the water was eventually evaporated through a defined number of clutch shifts.

Furthermore, Akita et al. [19] identified a correlation of water contamination and wear debris, that is, among other things, consisting of iron particles, with respect to low differential speed. This leads to an eventual decline of the CoF [19,27].

1.2. Research Objective

The objective of the present study is to accentuate critical factors that contribute significantly to an early performance loss of the lubricant. This knowledge is inevitable to monitor the behavior of the lubricant, reduce adverse NVH effects in wet clutches, and avoid deficient lubrication. As a result of the NVH behavior, the induced vibrations can cause mechanical damage to the entire powertrain unit. Awareness of relevant lubrication performance factors paves the way for recycling the lubricant to prevent early-stage damage to various components. Concerning earlier investigations, the focus is on water contamination, iron particles resulting from wear, and energy input. The oil performance was exemplarily evaluated on wet clutch systems since they have the highest tribological requirements amongst other machine elements.

2. Experimental Setup and Methodology

2.1. Test Setup

Several experimental testing procedures have been established to determine the performance data of wet clutches. These approaches are distinguished by how closely related the experimental setup is to the actual application of the component. Thus, the accuracy of the test results differs according to the effort required by the respective testing procedures.

Field testing often involves a complicated as well as cost-intensive test setup along with appropriate boundary conditions. While focusing on one specific section of the powertrain unit, side effects caused by supplementary machine elements can occur and must be considered. In contrast, model tests reduce the complexity of the test setup to a minimum to save costs and time, as well as to increase the efficiency of the study. Component test rigs, ultimately, combine the advantages of a straightforward test setup and applicable measurement data with regard to the actual application of the tested machine element.

The investigations regarding fresh oil in the presented study were carried out on the in-house designed KLP-260 component test rig. For the purpose of this study, the KLP-260 was slightly adapted by adding a specific shudder unit between test chamber and shaft to reduce the torsional stiffness. The test rig can operate either in slip or brake mode. An overview of the test rig setup is illustrated in Figure 2. Figure 3 shows a photograph of the used component test rig.

The mechanical setup of the test rig can be divided into three main sub-assemblies. Firstly, the wet clutch consisting of steel and friction disks can be mounted onto the outer and inner carriers in the test chamber. The actual carriers are adapted for use in the test rig to create application-related boundary conditions and obtain preferably accurate friction behavior. While the outer carrier is fixed to the housing, the inner unit is screwed onto a particular shudder unit which is connected to the rotating shaft. This unit is designed to reduce the torsional stiffness of the shaft and aims for transmitting the shudder signal from the clutch to the respective encoders. A force-controlled, hydraulic piston applies the pressure. Regarding lubrication, the lubricant can either be supplied from above or injected via an oil nozzle in a radial direction from the inner side. The thermostat-controlled feeding oil temperature and the flow rate can be independently varied throughout a wide range. Secondly, the rotating shaft connects the testing unit to the two motors as well as two switchable flywheels to adjust the inertia of the system. Thirdly, the main drive, which is linked to the shaft via a belt drive and engaged through an electromagnetic clutch, accelerates the shaft with the flywheels to a defined speed and is then decoupled from the system in the brake shift mode. On the other hand, the creep drive operates in the engaged state of the clutch in the slip mode and can, therefore, withstand conditions with high induced torque measured by a load cell. An incremental encoder at the end of the shaft measures the rotational speed. Table 1 represents the relevant technical data of the test rig.

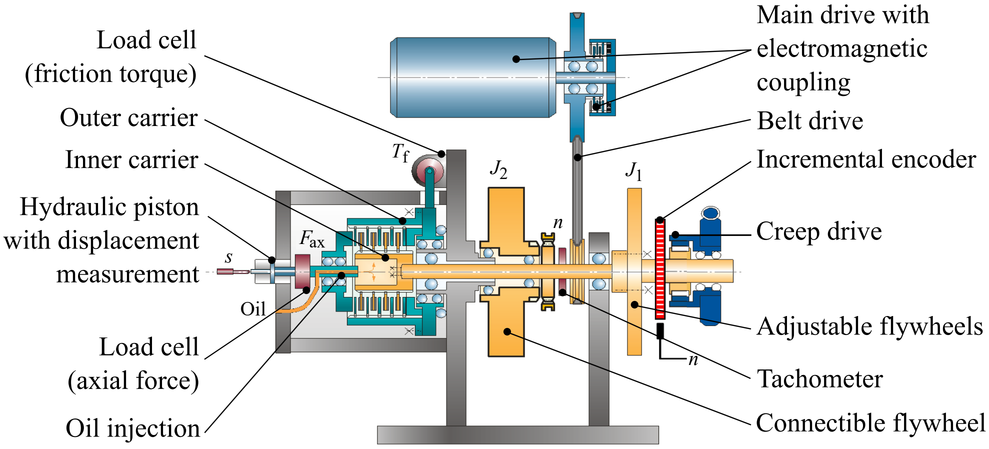

Figure 2. Schematic test rig setup of the KLP-260 component test rig according to Meingassner [28].

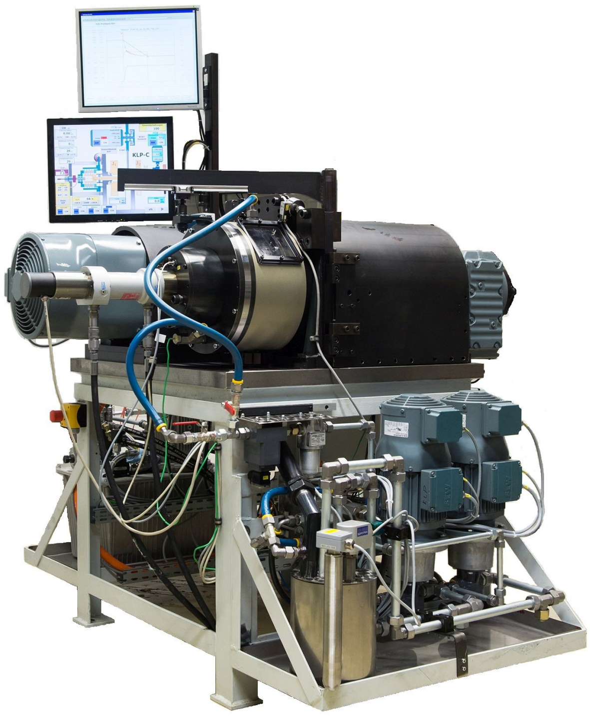

Figure 3. Photograph of the KLP-260 component test rig.

Table 1. Relevant technical data of the KLP-260 component test rig according to Meingassner [28].

	Parameter	Value
General	Maximum axial force	$F_{ax,max} = 40$ kN
	Disk dimensions	$d_o = 75 \ldots 260$ mm
	Oil temperature	$\vartheta_{oil} = 30 \ldots 150$ °C
	Oil flow rate	$\dot{V}_{oil} = 0 \ldots 7$ L/min
	Oil pressure	$p_{oil} = 0 \ldots 6$ bar
	Variable inertia	$J_1 = 0.12 \ldots 0.75$ kgm^2
	Basic inertia	$J_2 = 1.0$ kgm^2
Creep drive	Slip speed	$\Delta n = 0 \ldots 140$ rpm
	Max. torque	$T_{f,max} = 2000$ Nm
Main drive	Slip speed	$\Delta n = 0 \ldots 7000$ rpm
	Max. torque	$T_{f,max} = 60$ Nm

As shown in [29,30], the measurement accuracy of the KLP-260 is identified with regard to the rules of the Guide to the Expression of Uncertainty in Measurement (GUM) [31]. The determined uncertainty is illustrated in Table 2.

Table 2. Measurement accuracy of relevant technical parameters on the KLP-260 component test rig according to Strobl [29] based on Baumgartner [30].

Parameter	Measurement Uncertainty
Axial force	±1.3%
Torque	±0.4%
CoF	±1.3%
Slip speed (main drive)	±0.2%
Slip speed (creep drive)	±0.9%

To gain knowledge about the long-term behavior, tests were also performed with disks and oil samples originating from test rig and vehicle-based endurance runs to evaluate their friction behavior. Due to the minor oil volumes (<650 mL) available, these tests were carried out on a different component test rig (RRV). In contrast to KLP-260, the disks are mounted horizontally inside the RRV. A schematic setup of the test rig is given in Figure 4.

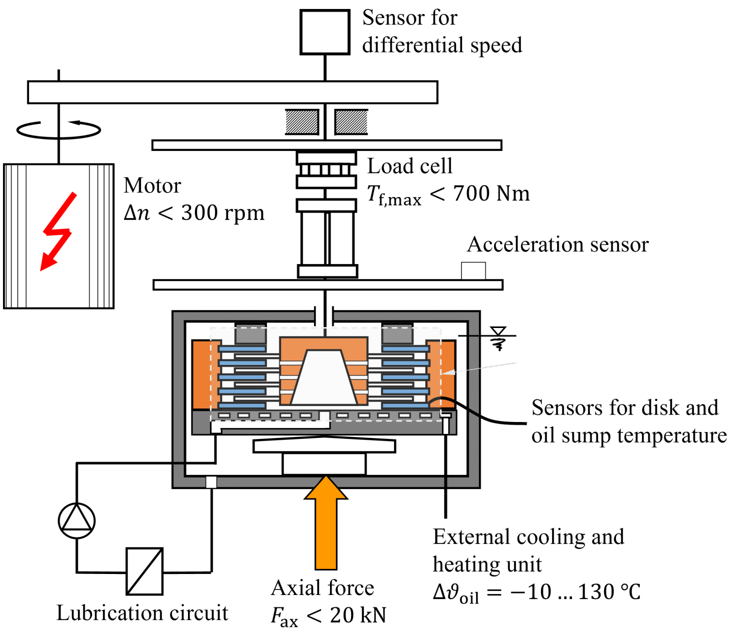

Figure 4. Schematic test rig setup of the RRV component test rig.

2.2. Operation Modes

Within the scope of these investigations, brake shifts, in general, can be neglected since all tests were performed in slip operation mode. On the one hand, slip shifts can occur at a constant differential speed (steady slip, e.g., overload clutches). On the other hand, the creep drive consecutively accelerates and decelerates over a one-second ramp multiple times in the transient slip mode, which finds use, for instance, in differentials. Both operation modes, including the course of the axial force (F_{ax}) and the differential speed (Δn) on KLP-260, are shown as an example in Figure 5. After each slip cycle, the axial force is temporarily released, and a pre-defined cooling sequence is run on KLP-260. For this purpose, the differential speed is set to $\Delta n = 100$ rpm and the axial force to $F_{ax} = 100$ N to ensure a uniform oil flow distribution through the grooves of the friction plate. This cooling phase persists until the average steel disk temperature is steady (∼45 s).

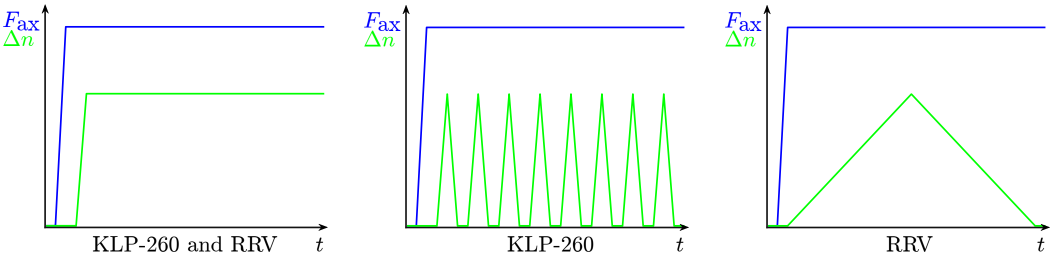

Figure 5. Course of the rotational speed Δn and the axial force F_{ax} in steady and transient slip modes.

2.3. Materials

For the experimental study, a friction pairing consisting of a stationary steel (outer) disk and a rotating friction (inner) disk with an organic, paper-based friction lining and a multi-segmented, radial groove pattern was used. Accurate mechanical properties of the friction material have not been measured within these investigations. However, studies with similar friction lining refer to a Young's modulus in the range from 27 to 100 MPa and an MRS roughness of approximately 6.0 µm [32–36]. Both disks are characterized by their mean diameter ($d_m = 116$ mm), and are applied in transfer cases used in serial automotive production. The radial width of the friction lining is approximately 18 mm. The nominal clearance between the two disks is 0.2 mm. An entire clutch pack consists of six steel disks and five friction disks, resulting in a total of ten friction interfaces ($z_{KLP} = 10$) in KLP-260. In contrast to that, RRV operates with four steel disks and three friction disks, adding up to six friction interfaces ($z_{RRV} = 6$). The disks are visualized in Figure 6.

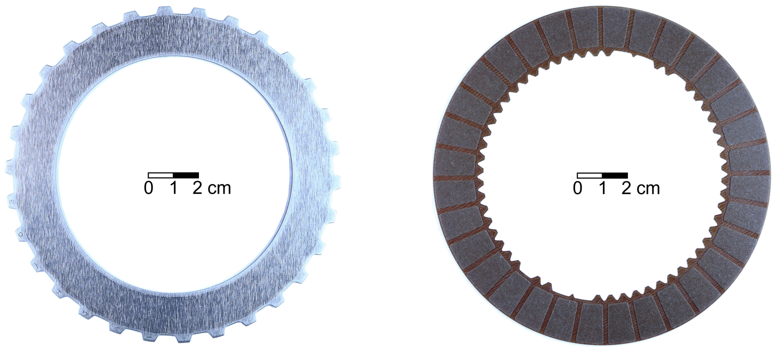

Figure 6. Steel (**left**) and friction disk (**right**) of size D116.

To investigate the thermal influences, a thermocouple (NiCrNi Type K Class 1) is placed within the center of an axially centered steel plate. The temperature gradient to the contact interface is assumed to be negligible due to the thermally conductive material of the steel disk and the insignificant distance (∼0.6 mm) [16]. Thus, the local mass temperature can be monitored throughout the shift cycle. The tip of the thermocouple is mounted with the addition of a thermally conducting paste containing a high-density poly-synthetic silver compound. A schematic sketch of the positioning can be obtained from Figure 7.

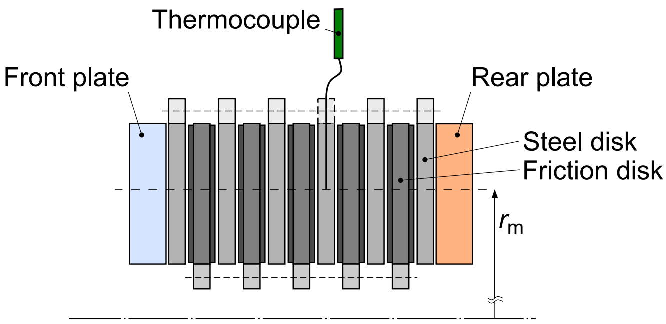

Figure 7. Positioning of a thermocouple within the center of the steel disk according to STROBL [29].

The L-204 fluid was used as a lubricant, which is commonly applied in automatic transmissions. The base oil comprises a mixture of group III (mineral oil) and IV (PAO). The technical data are listed in Table 3, and typical additive element contents are shown in Table 4. The lubricant is injected centrally into the inner carrier and amounts to 0.8 L per test. To recreate real ambient conditions, untreated rainwater was used within these tests.

Table 3. Technical data of the tested lubricant.

Lubricant	Kinematic Viscosity at 40 °C	Kinematic Viscosity at 100 °C
L-204	28 mm^2/s	6.0 mm^2/s

Table 4. Typical additive elements of the tested lubricant.

Lubricant	Ca	Mg	B	P	S
L-204	530 mg/kg	100 mg/kg	130 mg/kg	350 mg/kg	1600 mg/kg

The samples tested in the RRV component test rig—both disks and lubricant—originated from vehicle-based endurance runs. As in real-life application, the lubricant supported several wear-producing tribosystems, such as gears. The energy input was defined as the energy produced in the clutch. As vehicles may use different oil quantities, the specific energy input is given in kWh/L. These tests were performed with either adequate or inadequate water contamination according to the specifications of the manufacturer. The respective iron content of the oil samples was measured by inductively coupled plasma optical emission spectrometry (ICP-OES). Results are given in mg/kg.

2.4. Test Procedure

To avoid the presence of non-linear effects in the early lifetime phase, a pre-defined sequence of 100 run-in cycles (R1) in steady slip mode is executed. This step is taken after the lubricant has been supplied into the component test rig and the disks have been mounted onto the respective carriers into the inspection chamber. In this phase, a uniform axial pressure and a differential speed, according to Table 5, is applied to the friction pairing system. As the first action of a recurrently performed cycle, a pre-defined amount of water is added to the lubricant. After that, the lubricant is circulated for 15 min to ensure a homogeneous distribution of the added water amount [16]. Through different analyses in pre-tests, it is determined that the added water is evenly distributed in the lubricant after merely 10 to 15 min. Then, a specific sequence of ten steady (S1) and transient slip (T1) is run, respectively. After completion, the water is entirely evaporated by an additional 90 cycles of steady slip (S2), allowing for the observation of the designated friction behavior. The respective parameters are provided in Table 5. The pressure and differential speed are chosen according to application-related conditions. A schematic test procedure can be obtained from Figure 8.

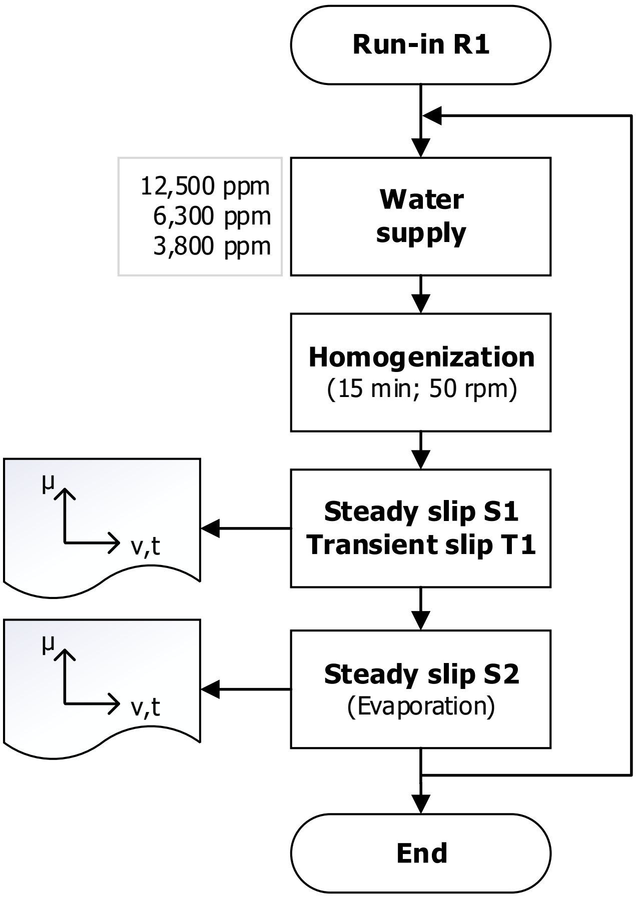

Figure 8. Test procedure to investigate the influence of water contamination on the performance of the lubricant at different water levels in KLP-260.

Table 5. Parameters of steady and transient slip sequence.

Name	Test Rig	Pressure p	Differential Speed Δn	Number of Slip Phases	Iterations
R1	KLP-260	1.0 MPa	100 rpm	1	100
S1	KLP-260	1.0 MPa	100 rpm	1	10
T1	KLP-260	1.0 MPa	100 rpm	8	10
S2	KLP-260	1.0 MPa	100 rpm	1	90
S3	RRV	0.5/1.0/2.0 MPa	10/15/20/25 rpm	1	3
T3	RRV	0.5/1.0/2.0 MPa	100 rpm	1	3

In each test on the RRV component test rig, different operation points were investigated. In steady and transient slip mode, shifts with axial pressure of 0.5, 1, and 2 MPa and at different temperature levels ranging from 30 °C to 90 °C were performed. The total test duration was up to 30 s. The test program started at 30 °C with the lowest rotational speed of 10 rpm, applying all three pressure stages in the steady slip mode (S3). After that, the rotational speed was consecutively increased. Subsequently, the same test procedure was carried out in transient slip mode (T3). After completion, the behavior at the next higher temperature level was repetitively investigated. To evaluate the shudder behavior, the test point at 30 °C in the transient slip mode was used. A schematic test procedure of the used disks and lubricants can be obtained from Figure 9.

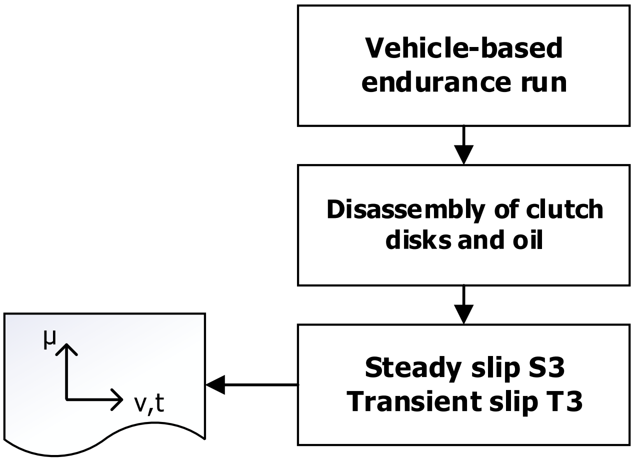

Figure 9. Procedure to evaluate the friction and shudder behavior of lubricants and disks out of vehicle-based endurance runs in the RRV component test rig.

3. Results

In the following section, the impact of three key factors on the performance loss of the lubricant are described in further detail. Therefore, the reversible and irreversible effects of water contamination and the correlation of iron particles with specific energy input with the performance of the lubricant are examined.

3.1. Effects of Water Contamination

Figure 10 illustrates a steady slip shift lasting approximately seven seconds without water addition. The axial force (blue) is applied immediately before launching the creep drive, accelerating the shaft to the designated speed (green). Furthermore, the red graph showcases the course of the torque. The CoF (pink) is calculated based on the torque and proportional to it. The resulting steel disk temperature is shown in black.

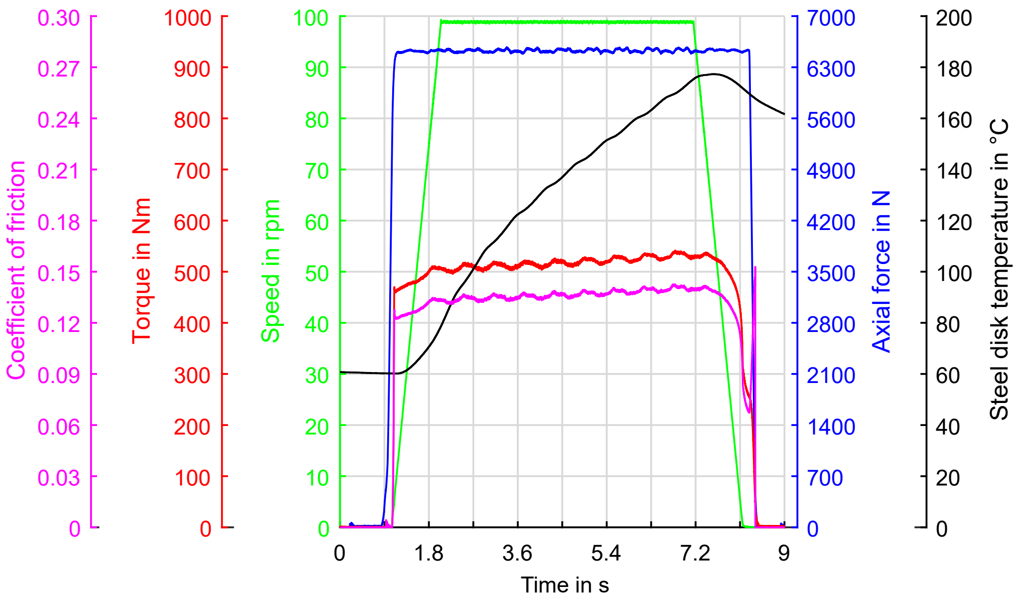

Figure 10. Example of a shift in steady slip mode tested in the KLP-260 component test rig.

As shown in Figure 11, severe shudder emerges in the first shift after the addition of water. In this particular case, the supplied water content of 12,500 ppm significantly exceeds the threshold value that the lubricant can compensate, according to the specifications of the manufacturer. In fact, the saturation point of the lubricant accumulates to less than 10% of the added amount, and the investigation was performed solely for scientific purposes. Evidently, enormous oscillations in the CoF curve accompanied by clearly audible NVH occur right after the engagement of the clutch. As a matter of fact, local torque peaks greater than 1000 Nm arise, which is double the value compared to the configuration without water addition. Consequently, the rise in the steel disk temperature increases according to the higher induced torque.

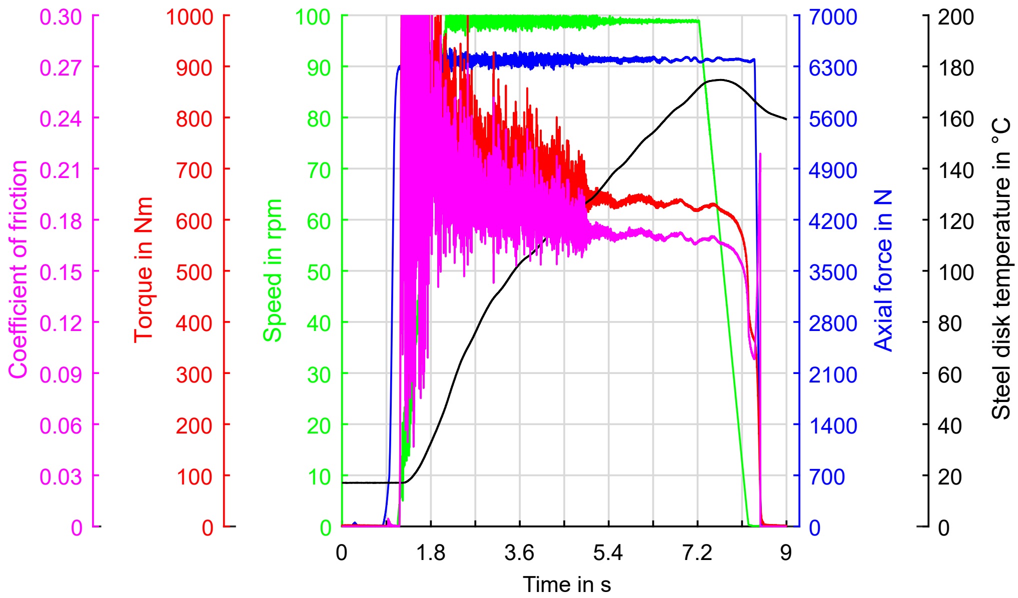

Figure 11. Severe shudder immediately after water addition (12,500 ppm) in steady slip mode tested in the KLP-260 component test rig.

Figure 12 shows the course of a typical transient slip shift where the rotational speed alternates. To achieve a comparable temperature rise compared to the one observed in the steady slip shift, eight slip phases are executed. Therefore, the creep drive accelerates and decelerates the system with a one-second ramp, while the axial force remains constant over the entire cycle. The number of slip phases was selected such that the wave-like temperature rise roughly equals the level of a steady slip shift.

In the transient slip mode, the shudder behavior of the clutch after water addition, imaged in Figure 13, resembles the steady slip observance: severe shudder appears with the engagement of the clutch. Taking both steady and transient shudder shifts into consideration, two principal effects emerge. Firstly, the level of the CoF and, thus, the induced torque significantly exceed the level of the initial configuration without water addition. Secondly, the occurring oscillations diminish with an incremental duration of the shift for steady as well as transient slip mode. Conclusively, it appears that water contamination impairs the performance of the lubricant. Moreover, the question arises as to whether the previous friction behavior can be fully restored after evaporation of the added water, along with its effects, or whether irreversible consequences remain.

To further investigate a potential answer to these two questions, the course of the CoF resulting from two steady slip shifts under the same boundary conditions is superimposed in Figure 14 with one exception. While the lower pink graph illustrates the reference configuration as previously shown, the upper curve represents the CoF under the addition of water. Obviously, water contamination leads to a significant increase in the CoF under the same operating conditions from $\mu \approx 0.14$ at the reference shift to $\mu \approx 0.16$. Moreover, the increase averages roughly $\Delta\mu = 18\%$ at a contamination level of 3800 ppm. However, it must be emphasized that the supplied water amount intentionally exceeds the saturation limit of the lubricant provided by the manufacturer. The added water contributes to a performance loss of the lubricant in a way that oil additives, such as friction modifiers

(FMs), are inhibited from performing their intended task, influencing the friction behavior of the clutch. Hence, critical water amounts over the saturation limit prevent the tribo-layer between the disks from fully establishing.

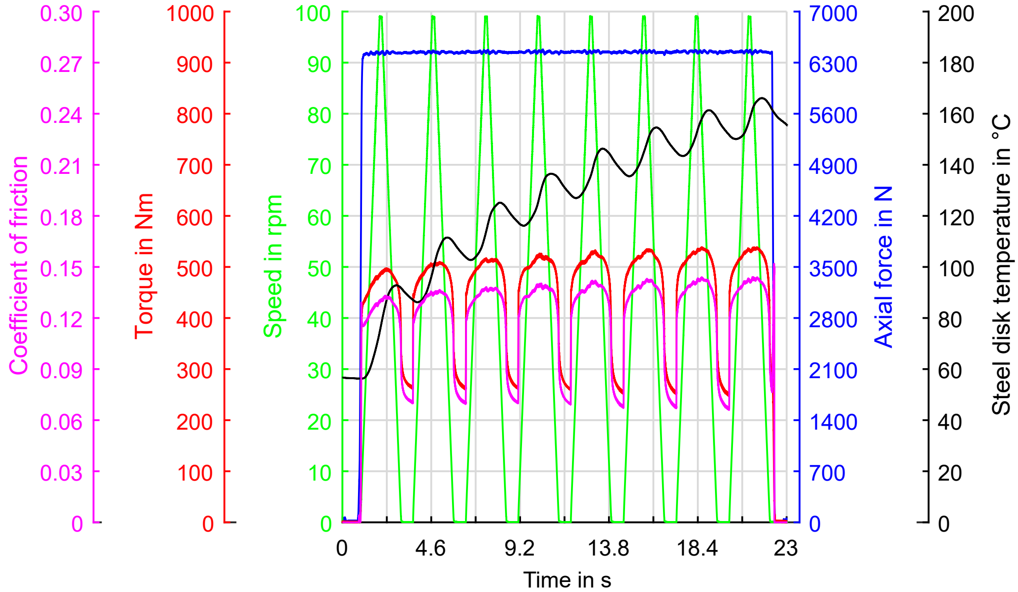

Figure 12. Example of a shift in transient slip mode tested in the KLP-260 component test rig.

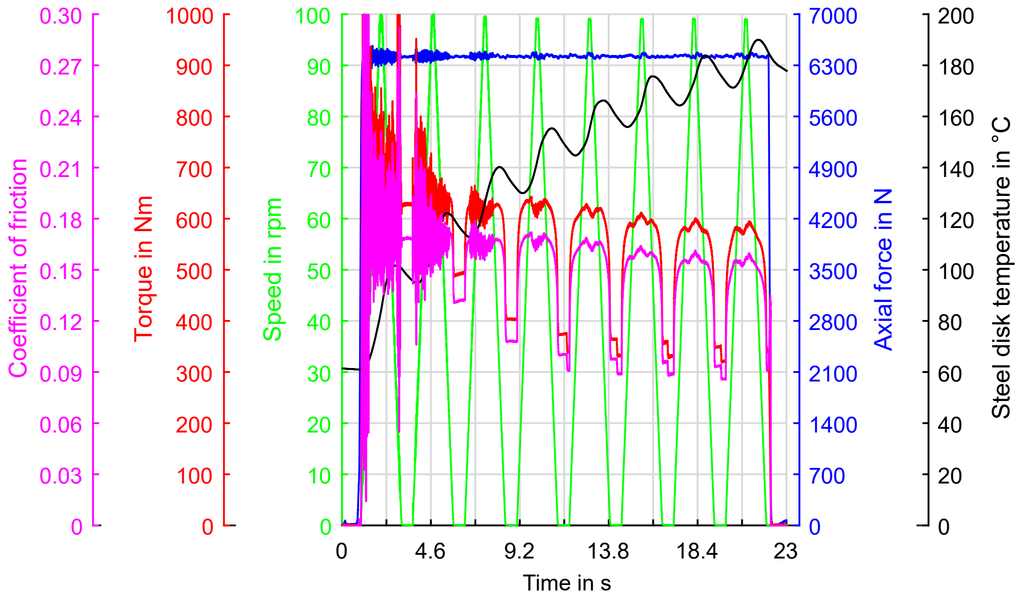

Figure 13. Severe shudder after immediate water addition (12,500 ppm) in transient slip mode tested in the KLP-260 component test rig.

To further investigate this influence, the added water amount was gradually increased from 3800 ppm to 6300 ppm, and finally, to 12,500 ppm. Figure 15 illustrates the CoF versus the sliding speed evaluated at the declining slope of the fifth slip phase in the transient slip mode. The black curve shows the behavior without water, and the blue graph represents the same added water amount as previously indicated. The CoF curve rises as expected with a further increase in the supplied water amount. The curve does not increase further after doubling the water amount to 12,500 ppm. In conclusion, the friction behavior is significantly influenced by the water content in the lubricant, ranging from the saturation limit of the lubricant to a point where the introduced contamination no longer has any additional impacts on the increase in the CoF.

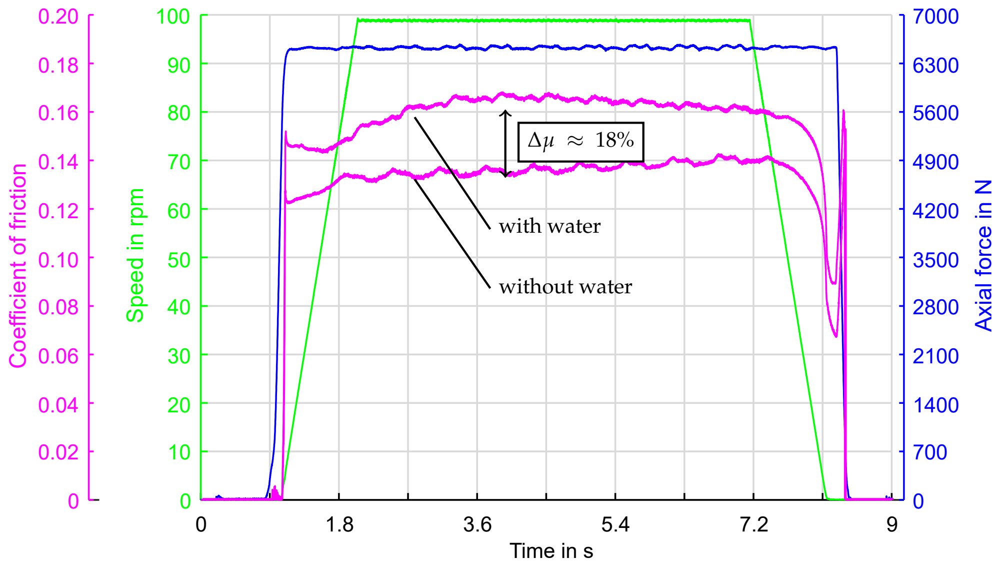

Figure 14. Course of the CoF without water versus with water addition (3800 ppm) tested in the KLP-260 component test rig.

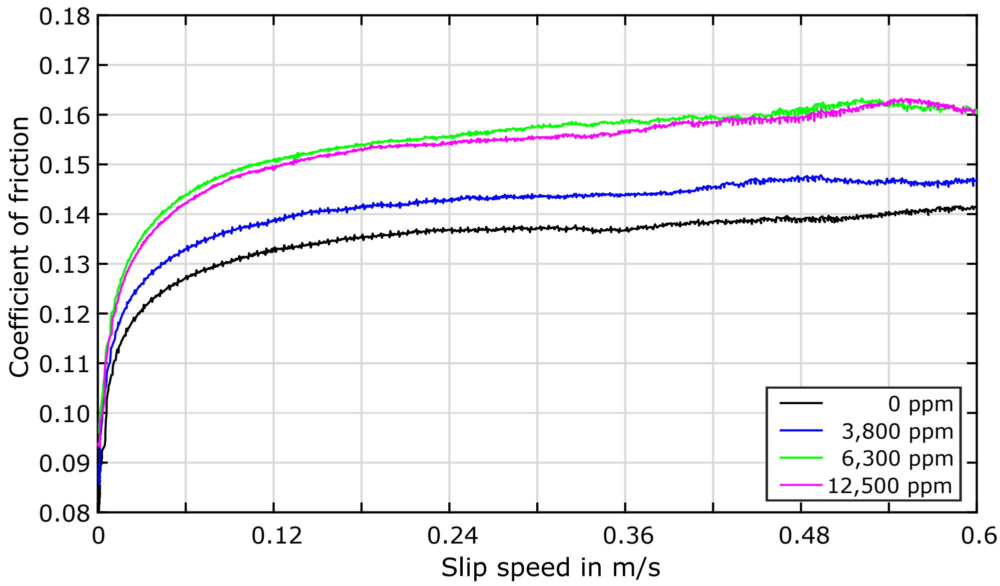

Figure 15. Course of the CoF with respect to the slip speed at different added water contents tested in the KLP-260 component test rig.

Eventually, to study irreversible changes in the friction behavior, the CoF is plotted in Figure 16 after entirely evaporating the water. Unlike immediately after water addition, where the CoF is significantly higher than without water, it decreases irreversibly after evaporation. This occurs independently from the amount of water that was induced into the lubricant.

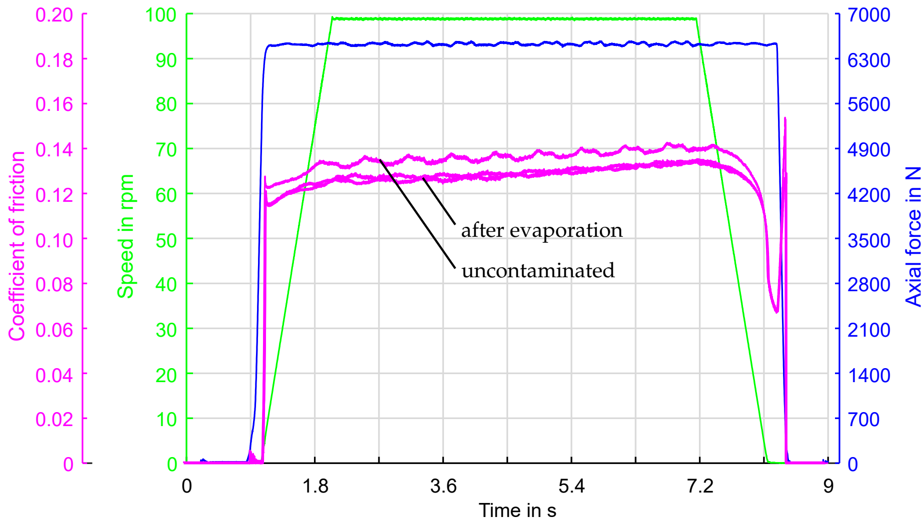

Figure 16. Course of the CoF after evaporation of different added water contents tested in the KLP-260 component test rig.

3.2. *Influence of Iron Particles and Energy Input*

Iron particles resulting from the wear and abrasion of various machine elements contribute to impairing the performance of the lubricant. In wet clutch systems, this degradation can lead to the presence of NVH behavior. To examine the influence of iron particles, as well as the correlation to specific energy input, oil samples out of vehicle-based endurance runs under high specific mechanical stress were investigated. These oil samples were eventually compared within the RRV component test rig. As part of this process, a specific amount of water, considered either adequate or inadequate according to the specifications of the manufacturer, was added to the lubricant.

Table 6 lists the parameters of vehicle-based endurance tests and provides information about the results of the evaluation in the RRV component test rig regarding shudder behavior. The average CoF ranges from 0.140 to 0.156. Exemplary shifts for test sample number 4 and test sample number 7 are illustrated in Figures 17 and 18, respectively. Both shifts were run on the RRV component test rig with 2 MPa axial pressure and 100 rpm maximum rotational speed. The oil sump temperature was set to 30 °C.

Table 6. Specifications of the tested lubricants in the RRV component test rig.

Sample Number	Water Contamination	Specific Energy Input	Iron Content	CoF at 30 °C and 2 MPa	Occurrence of Shudder
1	inadequate	68 kWh/L	440 mg/kg	0.151	no shudder
2	inadequate	7 kWh/L	436 mg/kg	0.141	shudder
3	inadequate	12 kWh/L	589 mg/kg	0.141	shudder
4	inadequate	7 kWh/L	493 mg/kg	0.140	shudder
5	adequate	4 kWh/L	183 mg/kg	0.145	no shudder
6	adequate	173 kWh/L	248 mg/kg	0.152	no shudder
7	adequate	58 kWh/L	838 mg/kg	0.156	shudder

The detailed friction and shudder behavior is shown exemplarily for two selected samples in Figures 17 and 18. Both diagrams represent a transient slip shift, where the rotational speed (green) is increased from 0 rpm to 100 rpm over a 10 s ramp and then decreased. The axial force (blue) is continuously applied. The black curve shows the temperature measured inside the steel disk. The CoF (pink) is calculated based on the torque and is proportional to it. Sample number 4 in Figure 17 with inadequate water contamination and 493 mg/kg iron content in the vehicle-based endurance run results in severe shudder in the RRV component test rig. This can be obtained from the enormous oscillations in the CoF curve. On the contrary, during the test stage of sample number 7 in the RRV component test rig in Figure 18 with adequate water contamination and 248 mg/kg iron content in the vehicle-based endurance run, no shudder behavior emerges.

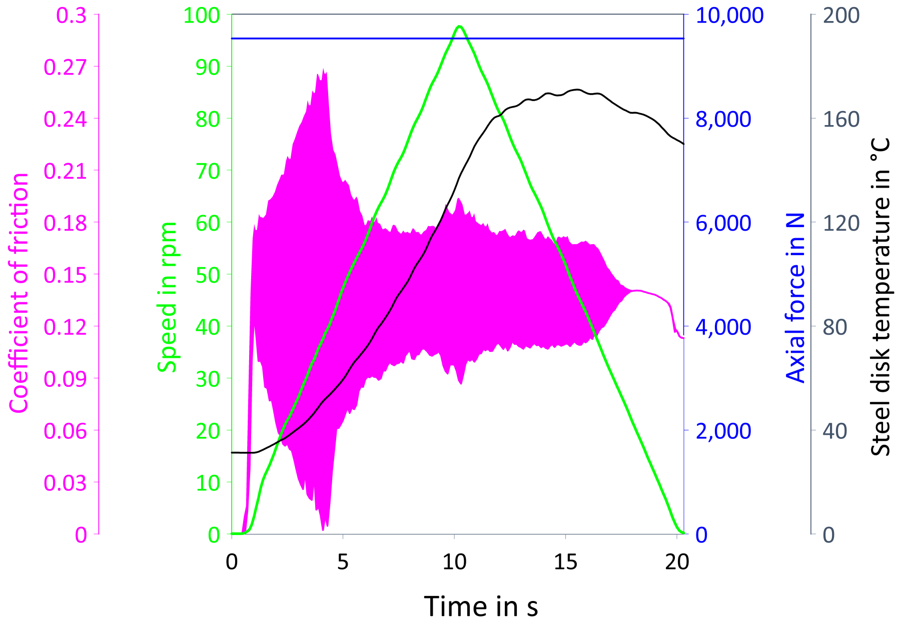

Figure 17. Friction behavior of sample number 4 (inadequate water contamination, shudder) tested in the RRV component test rig.

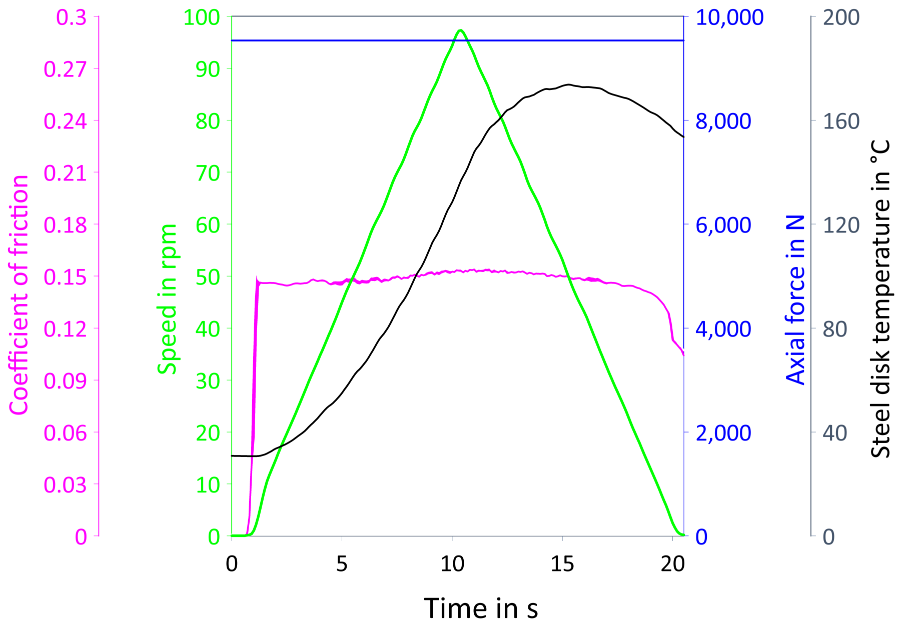

Figure 18. Friction behavior of sample number 7 (adequate water contamination, no shudder) tested in the RRV component test rig.

Figure 19 contains the tested oil samples with their respective iron content and energy input. Inadequate water contamination is visualized with green circles, whereas blue triangles represent the addition of an adequate water amount. The red circles highlight oil samples that showed shudder behavior.

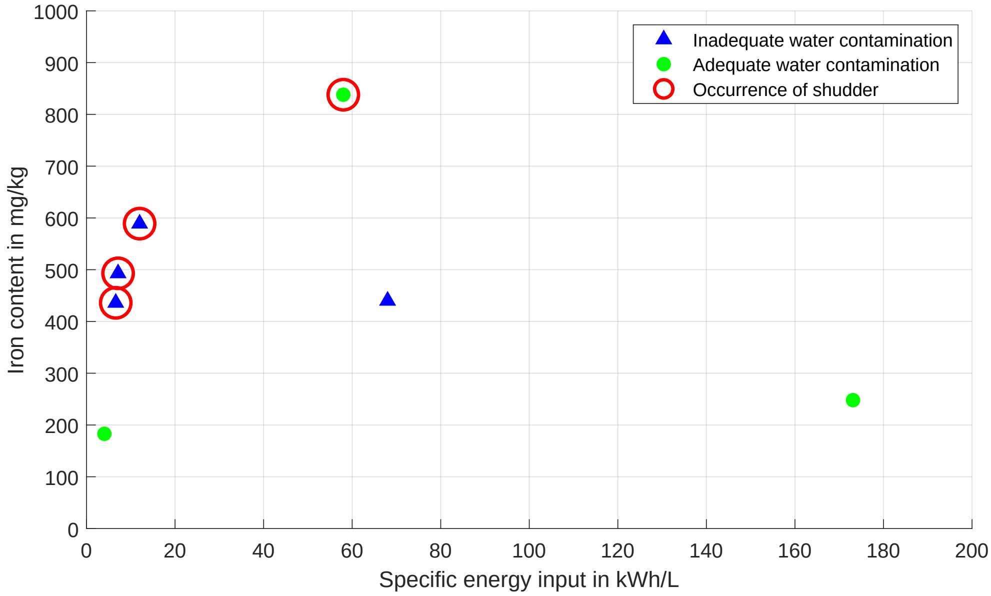

Figure 19. Occurrence of shudder with regard to iron content and specific energy input of oil samples out of vehicle-based endurance runs tested in the RRV component test rig.

4. Discussion

The observed changes in the friction behavior of wet clutches result from the degradation of the lubricant associated with water contamination. Generally, the chemical structure of additives, such as friction modifiers, dispersants, or detergents, consists of a polar head and a hydrocarbon tail. In an uncontaminated environment, the polar head of friction modifiers is attracted to the metal surface of the steel disk through adsorption forces [37,38]. The CoF between the friction interfaces increases by forming multi-molecular clusters via van der Waal forces. Due to their strong polarity, water molecules occupy the position on the steel disk, hindering the dedicated friction modifier molecules from forming the designated tribo-layer [39]. As a consequence, the friction level rises, and shudder occurs as observed in Figures 11, 13 and 14. However, with cumulative evaporation, this effect diminishes reversibly. Furthermore, the addition of water can also lead to secondary effects. The strongly polar water molecule contributes to building reverse micelles as additives are physically adsorbed by water molecules [40]. Due to the lack of freely available friction modifier molecules, the CoF decreases irreversibly as shown in Figure 16. Conclusively, water has a short-term influence on the friction behavior of wet clutches, as it causes adversities, such as shudder. Additionally, it contributes to the degradation of the lubricants via secondary effects.

The obtained perceptions from this study regarding the influence of water contamination corroborate the conclusions drawn in previously performed investigations. Refs. [16,18–20] emphasize a correlation between water contamination and a negative gradient of the CoF versus the sliding speed, resulting in undesirable NVH behavior.

Figure 19 correlates the impact parameters iron and water content with the specific energy input. Comparing the two samples with the lowest iron content and, in addition, adequate water content, it can be seen that both show no occurrence of shudder, although the specific energy differs significantly. In fact, one sample corresponds to the sample with the lowest specific energy input of 5 kWh/L, and the other with the highest of 173 kWh/L. This underlines the suggestion that the specific energy input has a lower impact on the shudder behavior of systems than the other presented parameters. With rising iron content, increased shudder tendency was detected, which is not always related to inadequate water content, e.g., one system with 840 mg/kg of iron but adequate water contamination showed shudder. This finding supports the assumption that samples with elevated iron content exhibit degraded tribological behavior even without the influence of water. However, most systems with inadequate water contamination and high iron content showed shudder in the tests, although the individual input of specific energy was low. One exception was the system with inadequate water contamination and the relatively high energy input of 68 kWh/L. Here, no shudder occurred. This corroborates the statement that the respective energy input is a parameter with low impact on the system performance, and higher input of energy does not automatically mean worse shudder behavior. Thus, it can be concluded that iron and water contamination, as well as their correlation, are the crucial factors contributing considerably to an early shudder tendency of the system.

Hence, the knowledge of existing studies on the influences of wear debris [19,27] was specified by determining iron particles being the main contributor to the performance loss of the lubricant. Moreover, a possible correlation between wear debris, or iron particles in particular, and water contamination, which was initially detected by Akita [19] through different model tests, was given proof by expanding the testing to a full component level.

5. Conclusions

The present study examined the impact of water contamination, iron particles, and energy input on the degradation of lubricants and the resulting effects on the friction behavior as well as the tendency to shudder of wet clutches. The following conclusions can be drawn from this paper:

- Water as a contaminant inhibits additives in the lubricant from performing their intended function by building reverse micelles with additive molecules and adsorbing on the metallic surface of the steel plate [40].
- Thus, water addition leads to an instantaneous increase in the CoF. After evaporation, irreversible changes persist, as the CoF tends to be lower compared to an uncontaminated lubricant.
- Significantly high water levels tend to cause shudder behavior of the clutch, resulting in NVH issues or early-state damage of machine elements.
- Tests with oil samples out of vehicle-based endurance runs have underlined that iron particles, as well as their correlation to water contamination, contribute inherently to a performance loss of the lubricant. At the same time, the influence of the energy input is secondary.

Author Contributions: Conceptualization, J.W., M.B., A.L. and H.P.; methodology, J.W., L.P.-G. and K.V.; validation, J.W., M.B., A.L. and H.P.; investigation, J.W., A.L. and C.B.; resources, M.B., C.B. and K.S.; data curation, J.W. and A.L.; writing—original draft preparation, J.W. and A.L.; writing—review and editing, J.W., C.B., L.P.-G., T.S. and K.S.; visualization, J.W.; supervision, H.P., K.V. and T.S.; project administration, M.B.; funding acquisition, M.B., A.L., K.V., H.P. and K.S. All authors have read and agreed to the published version of the manuscript.

Funding: This work was funded by the "Austrian COMET-Program" (project InTribology1, no. 872176) via the Austrian Research Promotion Agency (FFG) and the federal states of Niederoesterreich and Vorarlberg and was partly carried out within the "Excellence Centre of Tribology" (AC2T research GmbH).

Institutional Review Board Statement: Not applicable.

Informed Consent Statement: Detailed information about the chemical composition of the disks cannot be provided due to confidentiality requirements of the producer.

Data Availability Statement: The data presented in this study are available upon request from the corresponding author.

Acknowledgments: The authors would like to thank for the sponsorship and support of the Austrian Research Promotion Agency (FFG) and the federal states of Niederoesterreich and Vorarlberg and Magna Powertrain GmbH.

Conflicts of Interest: M.B. was employed by the company Magna Powertrain GmbH. A.L. was employed by the company AC2T research GmbH. C.B. was employed by the company AC2T research GmbH. The remaining authors declare that the research was conducted in the absence of any commercial or financial relationships that could be construed as a potential conflict of interest.

Abbreviations

The following abbreviations are used in this manuscript:

CoF	Coefficient of friction
FM	Friction modifier
ICP-OES	Inductively coupled plasma optical emission spectrometry
KLP	Kupplungs–Lebensdauer–Pruefstand (clutch lifetime test rig)
NVH	Noise, vibration, harshness
PAO	Polyalphaolefin
R	Run-in shift
RMS	Root mean square
RRV	Ring-Reibungs-und-Verschleiss Tribometer (ring friction and wear test rig)
S	Steady slip shift
T	Transient slip shift

References

1. Baese, M.; Lebel, A.; Franz, R.; Prost, J. Analysis of Wet Vehicle Clutch Damage Mechanism caused by Water. *Tribol. Schmier.* **2022**, *69*, 7–13. [CrossRef]
2. Bischofberger, A.; Ott, S.; Albers, A. Wet-Running Clutch as Actuator for Reduction of Oscillation in the Power Train—Influences of the Tribological System. *Forsch. Ingenieurwesen* **2020**, *85*, 1–10. [CrossRef]
3. Naunheimer, H.; Bertsche, B.; Ryborz, J. *Fahrzeuggetriebe: Grundlagen, Auswahl, Auslegung und Konstruktion*, 3rd ed.; Springer Veiweg: Berlin, Germany, 2019.
4. Hoehn, B.R.; Pflaum, H.; Mosbach, C. *Methodik zur Beurteilung des Schmierstoffeinflusses auf das Reibschwingverhalten Nasslaufender Lamellenkupplungen*; VDI Berichte: Dusseldorf, Germany, 2003; pp. 455–468.
5. Neumueller, M. Einfluss der Oelalterung auf Reibungs- und Verschleissverhalten von Synchronisierungen. Ph.D. Thesis, Technical University of Munich, Munich, Germany, 2001.
6. Mosbach, C. Das Reibungs- und Reibschwingverhalten Nasslaufender Lamellenkupplungen. Ph.D. Thesis, Technical University of Munich, Munich, Germany, 2002.
7. Kugimiya, T.; Yoshimura, N.; Mitsui, J. Tribology of Automatic Transmission Fluid. *Tribol. Lett.* **1998**, *5*, 49–56. [CrossRef]
8. Layher, M. Einfluss der Schmierstoffadditivierung auf das Reibungsverhalten Nasslaufender Reibschaltelemente. Ph.D. Thesis, Technische Universität München, München, Germany, 2011.
9. Miyazaki, M.; Hoshino, M. *Evaluation of Vibration-Preventive Properties of Lubricating Oils in Wet Friction Plates and Retation of such Properties Using a Friction Tester*; SAE Technical Paper No. 881674, SAE International, Warrendale, PA, USA, 1988; Volume 97, pp. 1061–1067. [CrossRef]
10. Nakada, T.; Nomura, T.; Yoshioka, T.; Nonoyama, M. *A Study of Additive Effects on ATF Frictional Properties Using New Test Methods*; SAE Technical Paper No. 902150; SAE International: Warrendale, PA, USA, 1990. [CrossRef]
11. Ohtani, H.; Hartley, R.J.; Stinnett, D.W. Prediction of Anti-Shudder Properties of Automatic Transmission Fluids Using a Modified SAE No. 2 Machine. *SAE Trans.* **1994**, *103*, 456–467.
12. Maeki, R.; Nyman, P.; Olsson, R.; Ganemi, B. *Measurement and Characterization of Anti-Shudder Properties in Wet Clutch Applications*; SAE Technical Paper No. 2005-01-0878; SAE International: Warrendale, PA, USA, 2005.
13. Zhao, H.; Morina, A.; Neville, A.; Vickerman, R. Anti-Shudder Properties of ATFs—Investigation into Tribofilm Composition on Clutch Friction Material and Steel Surfaces and the Link to Frictional Performance. *Tribol. Trans.* **2012**, *55*, 782–797. [CrossRef]
14. Hauser, C. Einfluss der Oelalterung auf Reibcharakteristik und Reibschwingverhalten von Lamellenkupplungen. Ph.D. Thesis, Technical University of Munich, Munich, Germany, 2006.
15. Bischofberger, A.; Ott, S.; Albers, A. Influence of Operating Parameters on the Vibration Reduction Effect in the Wet-Running Clutch System. *Forsch. Ingenieurwesen* **2021**, *85*, 933–944. [CrossRef]
16. Fatima, N.; Marklund, P.; Larsson, R. Water Contamination Effect in Wet Clutch System. *Proc. Inst. Mech. Eng. Part D J. Automob. Eng.* **2013**, *227*, 376–389. [CrossRef]
17. Fatima, N. Impact of Water Contamination and System Design on Wet Clutch Tribological Performance. Ph.D. Thesis, Lulea University of Technology, Lulea, Sweden, 2014.
18. Wang, H. *Effects of Water in All-Wheel-Drive Clutch Oil on All-Wheel-Drive Cornering Noise*; SAE Technical Paper No. 2022-01-5103; SAE International: Warrendale, PA, USA, 2022 . [CrossRef]
19. Akita, Y.; Abe, K.; Osawa, Y.; Goto, Y.; Nagasawa, Y.; Sugiura, N.; Wakamatsu, S.; Kosaka, K. *Analysis of Friction Coefficient Variation with Moisture between Friction Surfaces*; SAE Technical Paper No. 2016-01-0411; SAE International: Warrendale, PA, USA, 2016. [CrossRef]
20. Williamson, W.; Rhodillegible, B. *The Effects of Water on Cellulose-Based Frictional Surfaces in Automatic Transmission Clutch Plates*; SAE Technical Paper 961917; SAE International: Warrendale, PA, USA, 1996 . [CrossRef]
21. Baese, M.; Heipl, O.; Cokdogru, I.; Lipinsky, D.; Mallach, D.; Franz, R. Analysis of Wet Clutch Wear Mechanism with Tribological Tests and Time of Flight Secondary Mass Spectroscopy (ToF-SIMS). *Forsch. Ingenieurwesen* **2019**, *83*, 247–258. [CrossRef]

22. Fatima, N.; Marklund, P.; Mathew, A.P.; Larsson, R. Wet Clutch Friction Interfaces under Water-Contaminated Lubricant Conditions. *Tribol. Trans.* **2016**, *59*, 441–450. [CrossRef]
23. Engelhardt, C.M. Einfluss von Wasser in Getriebeoelen auf die Zahnflankentragfaehigkeit Einsatzgehaerteter Stirnraeder. Ph.D. Thesis, Technical University of Munich, Munich, Germany, 2019.
24. Barthel, A.J.; Al-Azizi, A.; Kim, S.H. Fundamental Understanding of Environmental Effects on Adhesion and Friction: Alcohol and Water Adsorption Cases. *Tribol. Lett.* **2013**, *50*, 157–168. [CrossRef]
25. Dorgham, A.; Azam, A.; Parsaeian, P.; Wang, C.; Morina, A.; Neville, A. An Assessment of the Effect of Relative Humidity on the Decomposition of the ZDDP Antiwear Additive. *Tribol. Lett.* **2021**, *69*, 72. [CrossRef]
26. *SAE No. 2 Clutch Friction Test Machine Guidelines*; SAE International: Warrendale, PA, USA, 2012.
27. Fernandes, G.; Zanotto, P.; Sinatora, A. The Role of Counter-Face Roughness on the Tribological Performance of a Clutch System Tested with a Pin-On-Disc Tribometer. *Lubricants* **2016**, *4*, 18. [CrossRef]
28. Meingaßner, G.J.; Pflaum, H.; Stahl, K. Test-Rig Based Evaluation of Performance Data of Wet Disk Clutches. In Proceedings of the 14th International CTI Symposium, Berlin, Germany, 7–10 December 2015; pp. 1–11.
29. Strobl, P.; Schermer, E.; Groetsch, D.; Pointner-Gabriel, L.; Voelkel, K.; Pflaum, H.; Stahl, K. Identification and Validation of Linear Friction Models Using ANOVA and Stepwise Regression. *Lubricants* **2022**, *10*, 286. [CrossRef]
30. Baumgartner, A. Reibungsverhalten Nasslaufender Lamellenkupplungen—Messunsicherheiten und Auswertemethoden. Master's Thesis, Technical University of Munich, Munich, Germany, 2020.
31. Shui, H.; Zhang, Y.; Yang, H.; Upadhyay, D.; Fujii, Y. Machine Learning Approach for Constructing Wet Clutch Torque Transfer Function. *SAE Int. J. Adv. Curr. Pract. Mobil.* **2021**, *3*, 2738–2744. [CrossRef]
32. Berger, E.J.; Sadeghi, F.; Krousgrill, C.M. Finite Element Modeling of Engagement of Rough and Grooved Wet Clutches. *J. Tribol.* **1996**, *118*, 137–146. [CrossRef]
33. Berger, E.J.; Sadeghi, F.; Krousgrill, C.M. Analytical and Numerical Modeling of Engagement of Rough, Permeable, Grooved Wet Clutches. *J. Tribol.* **1997**, *119*, 143. [CrossRef]
34. Gao, H.; Barber, G.C.; Shillor, M. Numerical Simulation of Engagement of a Wet Clutch with Skewed Surface Roughness. *J. Tribol.* **2002**, *124*, 305–312. [CrossRef]
35. Gao, H.; Barber, G.C. Microcontact Model for Paper-Based Wet Friction Materials. *J. Tribol.* **2002**, *124*, 414–419. [CrossRef]
36. Kimura, Y.; Otani, C. Contact and Wear of Paper-Based Friction Materials for Oil-Immersed Clutches—Wear Model for Composite Materials. *Tribol. Int.* **2005**, *29*, 943–950. [CrossRef]
37. Crawford, J.; Psaila, A. Miscellaneous Additives. In *Chemistry and Technology of Lubricants*; Mortier, R.M., Orszulik, S.T., Eds.; Springer Science+Business Media: Berlin/Heidelberg, Germany, 1994; Volume 1, pp. 160–173.
38. Dorgham, A.; Azam, A.; Parsaeian, P.; Khan, T.; Sleiman, M.; Wang, C.; Morina, A.; Neville, A. Understanding the Effect of Water on the Transient Decomposition of Zinc Dialkyldithiophosphate (ZDDP). *Tribol. Int.* **2021**, *157*, 106855. [CrossRef]
39. Fatima, N.; Holmgren, A.; Marklund, P.; Minami, I.; Larsson, R. Degradation Mechanism of Automatic Transmission Fluid by Water as a Contaminant. *Proc. Inst. Mech. Eng. Part D J. Automob. Eng.* **2015**, *229*, 74–85. [CrossRef]
40. Colyer, C.C.; Gergel, W.C. Detergants/Dispersants. In *Chemistry and Technology of Lubricants*; Mortier, R.M., Orszulik, S.T., Eds.; Springer Science+Business Media: Berlin/Heidelberg, Germany, 1994; Volume 1, pp. 62–82.